Agricultural Water Management 243 (2021) 106414

Contents lists available at ScienceDirect

Agricultural Water Management

journal homepage: www.elsevier.com/locate/agwat

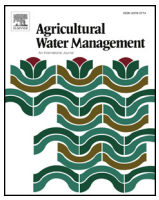

Higher canopy transpiration rates induced dieback in poplar (*Populus* × *xiaozhuanica*) plantations in a semiarid sandy region of Northeast China

Lining Song[a,b,c], Jiaojun Zhu[a,b,c,*], Ting Zhang[a,b,c], Kai Wang[d], Guochen Wang[e], Jianhua Liu[e]

[a] Key Laboratory of Forest Ecology and Management, Institute of Applied Ecology, Chinese Academy of Sciences, Shenyang 110016, China
[b] Qingyuan Forest CERN, Chinese Academy of Sciences, Shenyang 110016, China
[c] Key Laboratory for Management of Non-commercial Forests, Liaoning Province, Shenyang 110016, China
[d] College of Environmental Sciences and Engineering, Liaoning Technical University, Fuxin 123000, China
[e] Liaoning Institute of Sandy Land Control and Utilization, Fuxin 123000, China

ARTICLE INFO

Keywords:
Sap flow
Solar radiation
Vapor pressure deficit
Groundwater
Canopy conductance

ABSTRACT

Poplar (*Populus* × *xiaozhuanica*) plantations play an important role in controlling desertification in semiarid sandy regions of Northeast China, but their dieback occurs frequently in extreme drought years due to greater water loss by transpiration than water uptake. However, little is known about dynamics of canopy transpiration in poplar plantations, which limits our understanding of dieback mechanisms and proper management of these poplar plantations. Here, canopy transpiration and canopy conductance in 18-year-old poplar plantations were quantified by sap flow measurements in combination with monitoring of concurrent environmental variables during two consecutive growing seasons in normal and wet years (2018 and 2019). Results showed that daily canopy transpiration averaged 1.2 mm d^{-1} (between 0.3 and 1.9 mm d^{-1}) and 1.5 mm d^{-1} (between 0.2 and 2.4 mm d^{-1}) in 2018 and 2019, respectively. Solar radiation explained more variability of daily canopy transpiration than vapor pressure deficit (VPD) in both years, indicating that canopy transpiration was more controlled by radiation than by VPD. Total canopy transpiration during the growing seasons in 2018 and 2019 was 184.1 mm and 235.9 mm, respectively, accounting for 47.1 % and 44.2 % of precipitation over the same period. Sum of canopy transpiration, soil evaporation and change in soil water storage was higher than precipitation in most months, indicating that trees took up water from deep soil layer (> 1.0 m) and groundwater. Additionally, canopy conductance averaged 1.4 m s^{-1} and 1.9 m s^{-1} in 2018 and 2019, respectively, and decreased significantly with increasing VPD. However, sensitivity of canopy conductance to VPD decreased from 0.62 in 2018 to 0.27 in 2019, indicating a shift from more to less strict stomatal regulation. These findings indicate that poplar plantations are vulnerable to dieback during extreme drought years with decline in groundwater level due to utilization of groundwater for higher canopy transpiration rate.

1. Introduction

Water availability is the most limiting factor for tree survival and growth in semiarid and arid regions, where evaporative demand exceeds precipitation and available water resources are very scarce (Ayyoub et al., 2017; Wang et al., 2019). Climate models have predicted increases in air temperature together with increases in the frequency and severity of drought events in most arid and semiarid regions (Gao et al., 2018; Matusick et al., 2018). As a consequence, the water available for trees is likely to decrease, which will influence the tree physiological processes such as transpiration and related water use strategies that allow for tree growth and survival in semiarid and arid regions (Muñoz-Villers et al., 2018). As shown in recent studies, forest dieback and mortality worldwide are associated with global change-induced drought and heat (Anderegg et al., 2019; Flake and Weisberg, 2019; Ji et al., 2020). Therefore, it is urgently necessary to assess tree transpiration and how it shifts from its normal function in the semiarid and arid regions; such an assessment is essential for an understanding of tree survival strategies and water management. Moreover, understanding tree transpiration will also contribute to providing more mechanistic insights into tree responses to drought under global change scenario (Leo et al., 2013; Ungar et al., 2013; Sánchez-Costa et al., 2015).

Tree transpiration is a fundamental factor in understanding the ecophysiology of plantations and plays a crucial role in water budget in the arid and semiarid regions because it is the main component of

* Corresponding author at: Institute of Applied Ecology, Chinese Academy of Sciences, 72 Wenhua Road, Shenyang 110016, China.
E-mail address: jiaojunzhu@iae.ac.cn (J. Zhu).

https://doi.org/10.1016/j.agwat.2020.106414
Received 20 February 2020; Received in revised form 25 July 2020; Accepted 26 July 2020
Available online 05 August 2020
0378-3774/

evapotranspiration (Ungar et al., 2013; Tu et al., 2019; Wang et al., 2019; Tsuruta et al., 2019). The accurate quantification of tree transpiration is thus significant for tree physiology, ecohydrology, and other fields of study (Zhang et al., 2018a, Zhang et al., 2018b; Muñoz-Villers et al., 2018). The thermal dissipation method (Granier, 1987) is a commonly used method for measuring tree transpiration in various types of forests because it is easy to perform and is not limited by complex terrain or spatial heterogeneity (Hoelscher et al., 2018; Rana et al., 2020). In addition, the sap flux density measured by the thermal dissipation method can be scaled from representative individual trees to the stand level throughout the growing season (Bosch et al., 2014; Pasqualotto et al., 2019). Therefore, the sap flow method has been widely applied to quantify tree and stand transpiration. Tree transpiration is regulated by the behavioural responses of stomata to environmental drivers such as the vapor pressure deficit, solar radiation, soil water availability and precipitation (McDowell et al., 2008; Zhang et al., 2016; Tie et al., 2017). Stomatal control of transpiration exerts an important influence on the balance between carbon uptake and water losses, which influences tree survival and growth in arid and semiarid regions (Wieser et al., 2014; Urban et al., 2017; Muñoz-Villers et al., 2018). For instance, tree transpiration increases exponentially with the air vapor pressure deficit until a certain threshold at which the stomata close to maintain the water potential above a critical level. This constraint contributes to avoiding embolism, which jeopardizes the water-conducting system in trees (Zhang et al., 2017). Additionally, reduced soil water availability increases the hydraulic resistance between the soil and the root system, preventing water movement from soil to plant leaves, and triggers stomatal closure, avoiding or postponing hydraulic failure (Manzoni et al., 2014; Ghimire et al., 2018). Under such conditions, trees apply conservative water use strategies and appear to take up water from deeper soil layers and even from groundwater. Therefore, a better understanding of the impact of environmental drivers on tree transpiration is critical for revealing mechanisms of transpiration control and water use strategies in forests (Tie et al., 2017).

The Keerqin Sandy Land is one of the harshest desert areas in northern China and is also one of the key areas of the Three North Afforestation Programme (Great Green Wall) in China (Li et al., 2020; Song et al., 2020a). Poplar (*Populus* × *xiaozhuanica*), a hybrid of *Populus simonii* Carr. and *Populus nigra* L. var. *italica* Koehne, is a common tree species that is widely used to grow protective forests to control desertification in Keerqin Sandy Land because of its fast growth and high adaptability (Song et al., 2020a). These poplar plantations play an important role in controlling desertification and improving the local environment (Zheng et al., 2012; Song et al., 2020a). However, canopy dieback and mortality often occur in poplar plantations during drought years, which severely jeopardizes their ecological service functions. Previous studies have indicated that the water loss from transpiration being greater than the water uptake is the main cause of the canopy dieback and mortality in poplar plantations (Song et al., 2020a). However, the dynamics of transpiration in poplar plantations are still unknown. In addition, precipitation exhibits strong interannual variations in the Kereqin Sandy Land, and warming trends will continue (Song et al., 2016, Song et al., 2020a). Nevertheless, the effects of environmental drivers on transpiration in poplar plantations are still not fully understood. Therefore, it is vital to quantify canopy transpiration in poplar plantations and its response to environmental variables, to provide some suggestions for water management in these plantations to avoid dieback and mortality.

The objectives of this study were to 1) quantify canopy transpiration and canopy conductance in a poplar plantation in a semiarid sandy region during two consecutive growing seasons in normal and wet years (2018 and 2019), 2) determine the environmental and stomatal mechanisms of canopy transpiration control, and 3) determine the water-use strategies adopted by poplars.

2. Materials and methods

2.1. Study region

This study was conducted in the Zhanggutai region (42°43′ N, 122°22′ E, 226 m a.s.l.), Liaoning Province, China, which is located in the southeastern part of the Keerqin Sandy Land. This region is part of the semiarid climatic zone. The mean annual temperature is approximately 6.7 °C (mean value for 1954–2010). The annual mean precipitation and the annual mean pan evaporation is 474 mm and 1500 mm (mean value for 1954–2010), respectively (Song et al., 2020b). The major soil type is arenosols, in which soil particles with diameters ≥0.06 mm accounts for 94.0 % of the soil, and those with diameters < 0.06 mm account for 6.0 %. The average depth of the soil in the study region is approximately 107 cm (Zhu et al., 2003). The noncapillary porosity, capillary porosity and total porosity of the sandy soil are 0.02, 0.32 and 0.34 %, respectively. The field capacity of sandy soil is 17.5 % (Zhu et al., 2008). The groundwater levels were approximately 7.4 and 6.7 m in 2018 and 2019, respectively. The main tree species in the study region include *Pinus sylvestris* var. *mongolica*, *Pinus tabuliformis*, *P. xiaozhuanica* and *Ulmus pumila*. The area of poplar plantations occupies approximately 20 % of the total area of the Zhanggutai region (257 km^2) (Zheng et al., 2012). The species under the canopy of the plantations are annual grasses and herbs, such as *Potentilla anserina*, *Cleistogenes chinensis*, *Artemisia frigida*, and *Setaria viridis* (Song et al., 2016).

A 30 m by 30 m (900 m^2) plot within the poplar plantation (approximately 6.0 ha) was selected for the sap flow measurements. The poplar plantation was 18 years old in 2018. The tree density at the study site was 433 trees ha^{-1} in 2018 and 411 trees ha^{-1} in 2019 due to tree mortality. The mean stem diameter at breast height (DBH) was 16.7 cm in 2018 and increased to 17.3 cm in 2019. The mean tree height was 11.6 m in 2018 and 12.0 m in 2019. The mean leaf area index (LAI) was 0.56 m^2 m^{-2} and 0.60 m^2 m^{-2} during the growing seasons of 2018 and 2019, respectively. LAI was estimated by hemispherical photographs using a Nikon Coolpix 995 fitted with an FC-E8 fisheye lens (Song et al., 2020b). Five images in the plot were taken monthly using automatic exposure and upward-looking images 1.0 m from the ground avoiding midday hours.

2.2. Meteorological variable measurement

Meteorological variables, including the air temperature (T_a, °C), relative humidity (RH, %), precipitation (P, mm), wind speed (WS, m s^{-1}) and solar radiation (R_s, W m^{-2}), were measured and recorded continuously every 1 h in an automatic Zhanggutai weather station (approximately 3.0 km apart from the studied plot) during the measurement period. In addition to the above measurements, the air temperature and air relative humidity were also measured by a thermosensor (3688WD1; Spectrum Technologies, Inc., Aurora, USA) at 2.0 m height. Solar radiation was measured using a silicon pyranometer sensor (3670I; Spectrum Technologies, Inc., Aurora, USA) at 2.0 m height. These measurements were recorded every 10 min as averages by WatchDog 1000 series data loggers (Campbell Scientific, Logan, UT, USA) near the studied plot. The air vapor pressure deficit (VPD) was calculated from the air temperature and the relative humidity according to Campbell and Norman (1998).

The volumetric soil water content (θ, %) was continuously monitored at a single location with EC-5 sensors (Decagon, Inc. Decagon, USA) within the plot. The EC-5 sensors were installed at depths of 10 cm, 30 cm, 50 cm and 80 cm below the ground surface, which represented the soil layers of 0 − 20 cm, 20 − 40 cm, 40 − 60 cm, and 60 − 100 cm, respectively. However, θ data during the period from July 8 to July 29 in 2018 are missing due to equipment failure.

To reflect the interactive effects of climate drives on tree transpiration, the daily reference evapotranspiration (ET_o), an integrated

indicator involving radiation, wind speed, temperature, and vapor pressure deficit, was estimated by the Penman-Monteith equation in FAO-56 as follows based on the measured meteorological variables (Allen et al., 1998):

$$ET_o = \frac{0.408\Delta(R_n - G) + \gamma\frac{900}{T_a+273}U_2(e_s - e_a)}{\Delta + \gamma(1 + 0.34U_2)} \quad (1)$$

where R_n is the net radiation (MJ m^{-2} d^{-1}), which was estimated from the regression equation $R_n = 0.7965R_s$-57.64 (Zeppel et al., 2008); G is the soil heat flux density (MJ m^{-2} d^{-1}) (G was assumed to be negligible, i.e., G≈0, because the ground cover below the meteorological sensors was annual grasses and thus the magnitude of the daily average soil heat flux density was relatively low) (Allen et al., 1998; Tie et al., 2017); T_a is mean daily air temperature at 2 m height (°C); U_2 is the wind speed at 2 m height (m s^{-1}); e_s is saturation vapour pressure (kPa); e_a is actual vapour pressure (kPa); Δ is slope vapour pressure curve (kPa °C^{-1}); and γ is the psychrometric constant (kPa °C^{-1}).

2.3. Sap flow measurement and calculation of canopy transpiration

Sap flow measurements were conducted from May 1 to September 30 in 2018 and 2019 using Granier-type thermal dissipation probes (TDPs) (Granier, 1987). Each sensor consisted of a pair of probes 20 mm long and 2 mm in diameter, and a copper-constant thermocouple was placed in each probe. Based on the distribution of DBH (Fig. 1a), seven and eight trees were selected as sample trees in April 2018 and 2019, respectively (Table 1). All probes were inserted into the north-facing side of the trunk at a height of 1.3 m above the ground to minimize sun-exposure (Song et al., 2020b). To install the probes, the bark of the sample tree was removed until the cambium was exposed. The distance between the two probes was approximately 15 cm. The probes were mounted with waterproof silicone and covered with an aluminium box cover to avoid physical damage and solar radiation and to reduce the effects of ambient temperature fluctuation and rainfall (Shen et al., 2015; Tie et al., 2017; Song et al., 2020b). The temperature difference data between the heated and reference probes were recorded at 10 min intervals on a data logger (CR1000, Campbell Scientific Inc., Logan, UT, USA). The sap flux density (J_s) can be calculated according to the standard calibration for the TDP method (Granier, 1987):

$$J_s = 0.0119\left[\frac{\Delta T_m - \Delta T}{\Delta T}\right]^{1.231} \quad (2)$$

Table 1
Characteristics of sample trees of poplar plantation in 2018 and 2019.

No.	2018			2019		
	DBH (cm)	Tree height (m)	A_s (cm^2)	DBH (cm)	Tree height (m)	A_s (cm^2)
1	19.7	14.1	186.7	20.7	14.7	204.2
2	23.8	15.8	270.0	24.1	16.1	277.4
3	18.7	14.6	170.6	19.3	15.2	180.1
4	10.8	7.6	83.8	11.1	8.6	86.1
5	17.5	9.8	153.1	18.2	10.6	163.1
6	11.3	8.6	87.6	11.6	9.4	90.0
7	16.4	10.2	138.7	17.1	11.2	147.7
8				21.2	14.2	213.6

Note: DBH: diameter at breast height; A_s: sapwood area.

where J_s (g cm^{-2} s^{-1}) is the sap flux density, ΔT (°C) is the temperature difference between the two probes at any given time, and ΔT_m (°C) is the maximum temperature difference between probes, which was determined as the maximum value of daily ΔT_m over a 7–10 day period to avoid underestimation of the night-time sap flow (Lu et al., 2004). The thermal dissipation method has been demonstrated to be highly reliable for sap flow measurements of *Populus* spp. (Di et al., 2019). Therefore, it is believed to be valid for the poplars in the present study. As there was only one probe per sample tree, the azimuthal and radial variations in sap flux within the trees were not taken into account in this study; we assumed that these variations were low (Di et al., 2019). Although we did not directly measure the circumferential and radial variations in sap flux density for poplar (*Populus* × *xiaozhuanica*) in the present study, Su et al. (2010) measured the sap flux density at four depth in the xylem (i.e., 10, 20, 30, and 40 mm) of *Populus* × *xiaozhuanica* at the study site and found that there was no significant difference between the estimations of tree transpiration made from a single sensor at 20 mm and from the four integrated sensors at different depths. To accurately quantify tree transpiration in poplar (*Populus* × *xiaozhuanica*), the circumferential and radial variations in sap flux density should be investigated in the future. Based on the above assumption, the tree water consumption (*TWC*) can then be calculated as:

$$TWC = J_s \times A_s \quad (3)$$

where A_s is the sapwood area (cm^2). To determine the sapwood area, the staining method was applied to 12 trees outside the plot within the plantation (Chang et al., 2014). In each tree, increment cores were

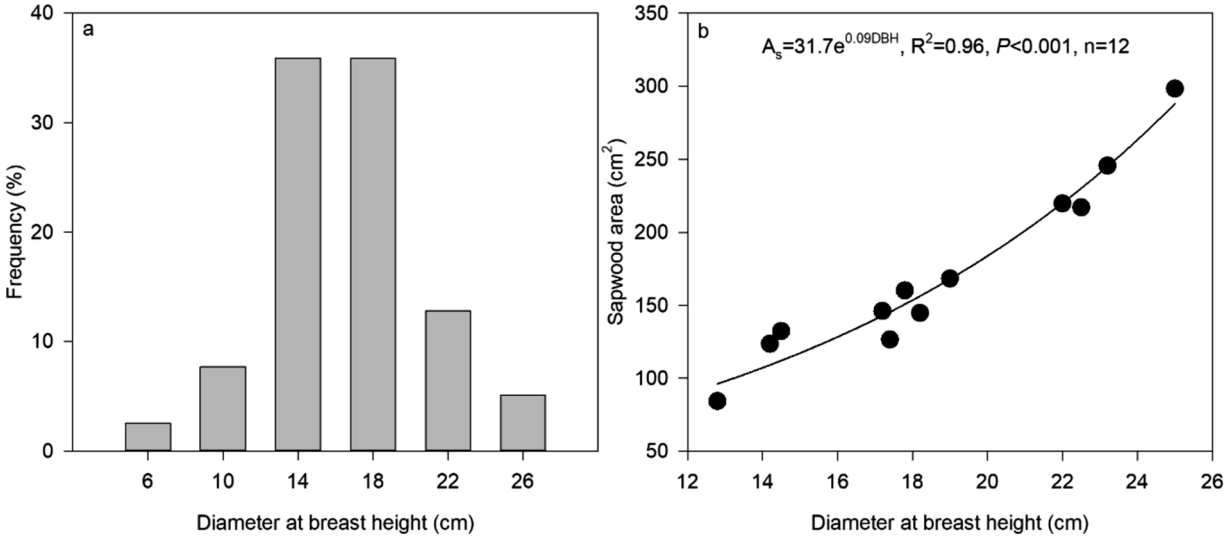

Fig. 1. Frequency distribution of tree diameters at breast height (DBH) values (a) and relationships between sapwood area (A_s) and diameter at breast height (b) in the poplar plantation.

drilled at a height of 1.3 m using an increment borer (5.15 mm), and water-soluble red dye (0.5 % acid fuchsin) was then injected into the drilled hole using a plastic pipette. After approximately 3–4 h, an increment core at approximately 3–4 cm above the initial hole in each tree was collected. The difference in color is clearly discernible, e.g., sapwood appears pink and wetter than heartwood. The sapwood thickness was measured with a ruler (precision of 1.0 mm), and the relationship between the sapwood area (A_s) and DBH was established (Fig. 1b).

The canopy transpiration per unit of ground area (E_c, mm d^{-1}) was calculated by multiplying the mean J_s for all the sample trees (J_{avg}) and the total sapwood area of the studied plot per unit of ground area (A_g) (Otieno et al., 2014; Song et al., 2020b).

$$J_{avg} = \frac{\sum_{i=1}^{n=7or8} J_{si} \times A_{si}}{\sum_{i=1}^{n=7or8} A_{si}} \quad (4)$$

$$E_c = J_{avg} \frac{A_{ts}}{A_g} \quad (5)$$

where J_{si} *is* the sap flux density of the ith sample tree; A_{si} is the sapwood area of the ith sample tree; A_{ts} is the total sapwood area in the studied plot, which was 6007.7 and 5952.6 cm^2 in 2018 and 2019, respectively; and A_g is the area of the studied plot (900 m^2).

During the 2018 and 2019 growing seasons, the sap flux was measured in the same trees, except that one sample tree was added in 2019 (Table 1). The quality of the sensor readings was regularly controlled, and if necessary, sensors were replaced. However, the power was failure during the period of September 11 and September 30 in 2019. The missing data accounted for approximately 6.9 % of all sap flow data across two years. Multiple linear regression between E_c and ET_o was applied to fill the missing gap (Zheng and Wang, 2014).

2.4. Canopy conductance

The canopy conductance (G_c, m s^{-1}) was calculated from the inverted Penman-Monteith equation as follows (Zhang et al., 2016; Xu et al., 2018):

$$G_c = \frac{\gamma \lambda E_c g_a}{\Delta R_n + \rho c_p VPD g_a - \lambda(\Delta + \gamma) E_c} \quad (6)$$

where λ is the latent heat of vaporization of water (2.45 MJ kg^{-1}); E_c is the canopy transpiration per unit of ground area (mm d^{-1}); Δ is the ratio of the saturated vapor pressure to temperature (kPa $°C^{-1}$); R_n is the net radiation (MJ m^{-2} d^{-1}), which was derived from the measured solar radiation at 2.0 m height using the formula $R_n = 0.7965R_s$-57.64 (Zeppel et al., 2008); ρ is the air density (kg m^{-3}), C_p is the specific heat of air (1.013 MJ kg^{-1} $°C^{-1}$); VPD is the vapor pressure deficit (kPa); γ is the psychrometer constant (0.067 kPa $°C^{-1}$); and g_a is the aerodynamic conductance (m s^{-1}) calculated from Eq. (7) (Monteith and Unsworth, 2013; Fu et al., 2020).

$$g_a = \frac{1 + 0.54U_z}{\left[\ln \frac{z-d}{z_o}\right]^2} \quad (7)$$

where U_z is the wind speed above the canopy (m s^{-1}), z is the wind speed measurement height (canopy height, m), z_o is the roughness height (usually 0.1 H and H are the canopy heights) and d is the displacement height (0.75 H) (Sommer et al., 2002; Xu et al., 2018). U_z was calculated from the measured wind speed at 2.0 m height based on Eq. (8) (Allen et al., 1998)

$$U_z = \frac{\ln(67.8z - 5.42)}{4.87} U_2 \quad (8)$$

To quantify the decoupling extent of stomata from the atmosphere, the decoupling coefficient (Ω) was estimated in the present study. Ω ranges from zero to one. When Ω approaches zero, stomatal control of the canopy transpiration is strong and a fractional change in canopy conductance leads to an equal fractional change in transpiration. Stomata exert less control on canopy transpiration as Ω approaches one; as a result, the canopy transpiration is controlled more by solar radiation and is less dependent on the atmospheric humidity deficit (Jarvis and McNaughton, 1986; Xu et al., 2018). The Ω can be calculated following Kumagai et al. (2004) and Fu et al. (2020):

$$\Omega = \frac{1}{1 + [\gamma/(\Delta + \gamma)](g_a/G_c)} \quad (9)$$

2.5. Measurement of changes in soil water storage and soil evaporation

To determine the water-use strategies of the plantation trees, the changes in soil water storage and soil evaporation were also measured in the present study. Soil water storage (S, mm) is calculated as

$$S = \sum_{i=1}^{n} \theta_i \times d_i \quad (10)$$

where θ_i is the volumetric soil water content of the ith layer (%), d_i is the thickness of the ith soil layer (cm) and n is the number of soil layers considered (n = 4). The change in soil water storage (ΔS) at a monthly scale was calculated as follows:

$$\Delta S = S_1 - S_2 \quad (11)$$

where S_1 is the soil water storage at the final stage (the last day of each month during the growing season) across the soil layer, and S_2 is the soil water storage at the beginning stage (the first day of each month during the growing season) across the soil layers.

In addition, soil evaporation was measured by a microlysimeter, which is a simple but effective method (Liu et al., 2017a). The microlysimeters were made of PVC-material (10 cm in internal diameter and 30 cm in height). The bottom of each micro-lysimeter was capped with a nylon net to allow the free drainage of water. Five microlysimeters were installed uniformly in the studied plot. The microlysimeters were weighed at the same time every day (i.e., approximately 19:00 pm) using an electronic balance with a precision of 0.1 g. For each lysimeter, the difference in the weights measured every 24 h (one day) is regarded as the daily evaporation from the soil. The soil in the microlysimeter was replaced with soil from the surrounding area every 5–7 days to prevent any interference from the cessation of water exchange with the subsoil caused by root activities (Liu et al., 2017a).

2.6. Data analysis

Significant differences in the micrometeorological variables (T_a, VPD, R_s, ET_o, θ) between the two growing seasons were tested using a paired samples *t*-test. To avoid the effect of stem capacitance on the analysis of transpiration responses to variations in environmental conditions, the 10 min average values of E_c and the environmental variables were averaged to the daily means (Wieser et al., 2014). The significant of differences in E_c, G_c and Ω between the two years were tested using the paired samples *t*-test. The relationship between E_c and θ was analysed by linear regression, whereas the relationships between E_c and VPD, R_s and ET_o were analysed by an exponential threshold model as below:

$$E_c = a(1 - e^{-bx}) \quad (12)$$

where *a* and b are the fitting parameters, E_c is the daily canopy transpiration and x is the corresponding meteorological variable.

The responses of G_c to *VPD* were examined using the following a linear logarithmic function (Oren et al., 1999):

$$G_c = -m \ln VPD + G_{cref} \quad (13)$$

where G_c is the canopy conductance, m is the stomatal sensitivity to VPD, and G_{cref} is the reference canopy stomatal conductance for *VPD* =

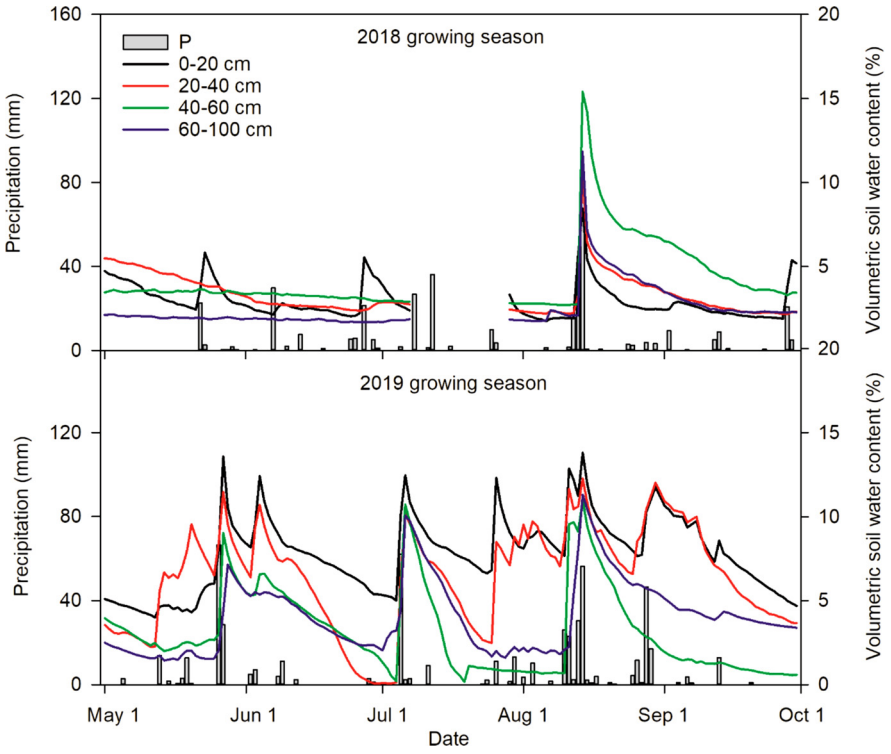

Fig. 2. Daily precipitation and volumetric soil water content (θ) at different depths (0–20 cm, 20–40 cm, 40–60 cm, and 60–100 cm) during the growing seasons in 2018 and 2019.

1 kPa (Ewers et al., 2001). ANCOVA was used to test for significant differences in -m and G_{cref} between the two years.

All statistical analyses were performed with SPSS 16.0 software package (SPSS Inc., Chicago, IL, USA).

3. Results

3.1. Microclimate and soil moisture

The total precipitation during the growing season (May-September) in 2018 and 2019 was 391.2 mm and 533.2 mm, respectively, accounting for 98 % and 133 % of the long-term average precipitation over the same period (401 mm, 1954–2010) (Fig. 2). This indicated that 2018 was a normal year while 2019 was a wet year. Since the topsoil was exposed to precipitation and evaporation, the θ in the upper layer increased quickly after precipitation events but decreased rapidly thereafter. As a result, the θ of shallow layers tended to be highly variable in both observed years. However, the θ of deeper soil layers was seasonally stable in 2018, whereas it exhibited similar changes to those in the shallow layers in 2019. The θ averaged 3.1 % and 5.2 % (weight-average) during the growing seasons of 2018 and 2019, respectively, ranging from 2.0 % to 11.7 % and from 2.2 % to 11.9 % (Fig. 2). A significant difference in θ was observed between the two years ($t = -11.3$, $P < 0.001$), with a higher value in 2019.

The air temperature (T_a) ranged from 8.3 to 34.8 °C in the growing season of 2018 and from 10.3 to 31.3 °C in the growing season in 2019, with the mean values of 23.8 and 23.0 °C, respectively (Fig. 3a). Significant differences in the daily mean T_a were observed in both years ($t = 2.13$, $P < 0.05$), with a higher value in 2018. The vapor pressure deficit (VPD) averaged 1.4 kPa and 1.2 kPa in the growing seasons of 2018 and 2019, respectively, ranging between 0.2 and 2.9 kPa and between 0.4 and 3.2 kPa (Fig. 3b). Significant differences in the daily mean VPD were observed in both observed years ($t = 2.90$, $P < 0.01$), with a higher value in 2018. The solar radiation (R_s) varied between 37.8 and 365.5 W m^{-2} and between 15.5 and 374.3 W m^{-2} in the growing seasons of 2018 and 2019, respectively, with mean values of 227.8 and 238.0 W m^{-2} (Fig. 3c). There was no significant difference in the daily mean R_s between two observed years ($t = -1.10$, $P > 0.05$). The reference evapotranspiration (ET_o) averaged 6.0 mm d^{-1} in both growing seasons, ranging from 0.9 to 11.3 mm d^{-1} in 2018 and from 1.2 to 12.0 mm d^{-1} in 2019 (Fig. 3d). No significant difference in mean daily ET_o was found between the two observed years ($t = 0.33$, $P > 0.05$). These data suggest that the weather was warmer and drier in 2018 than in 2019.

3.2. Sap flux density and canopy transpiration

The diurnal J_s during five representative days (mean values for seven sample trees in 2018) and the corresponding environmental variables are shown in Fig. 4. On sunny days, the sap flow generally increased from approximately 6:00 am, reached a peak value at approximately 9:00 am, and gradually decreased thereafter. Daily variations in J_s seemed to be associated with variations in T_a, VPD and R_s, e.g., J_s increased rapidly in the morning as the air temperature, VPD and R_s increased and reached a maximum, and J_s subsequently decreased.

The daily E_c reached an average of approximately 1.2 mm d^{-1}, with a maximum of approximately 1.9 mm d^{-1}, and a minimum of approximately 0.3 mm d^{-1} during the growing season in 2018 (Fig. 5). During the growing season in 2019, the daily E_c was between 0.2 and 2.4 mm d^{-1}, with a mean value of approximately 1.5 mm d^{-1} (Fig. 5). There was a similar monthly E_c change pattern between the two growing seasons. The maximum monthly E_c was 41.5 mm and 51.1 mm in May of 2018 and 2019, respectively, whereas the minimum monthly E_c was 31.2 mm and 41.4 mm in August of 2018 and 2019, respectively (Fig. 5 and Table 2). The accumulated E_c was 184.1 and 235.9 mm during the growing seasons in 2018 and 2019, respectively, accounting for 47.1 % and 44.2 % of the precipitation over the same period (Table 2). In addition, the precipitation was less than the sum of E_c, ΔS and soil evaporation in May, June, July, and September of 2018 and

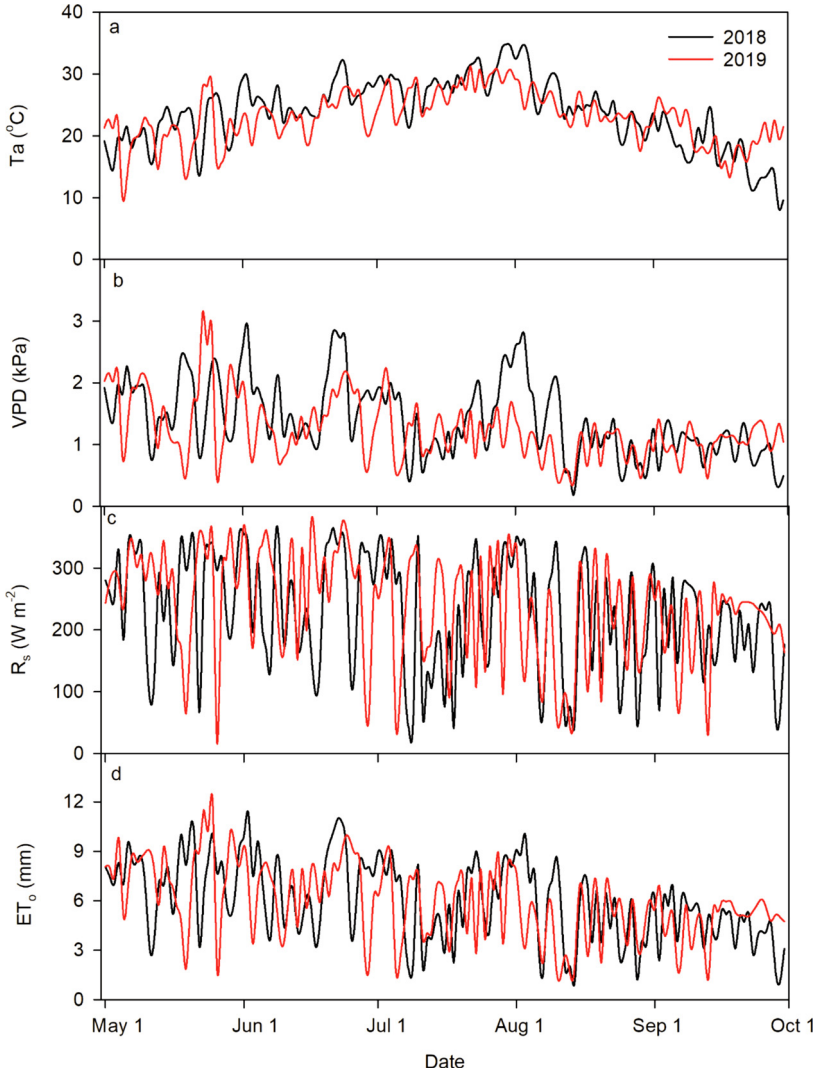

Fig. 3. Dynamics of daily air temperature (T_a, a), vapor pressure deficit (VPD, b), solar radiation (R_s, c) and reference evapotranspiration (ET_o, d) during the growing seasons in 2018 and 2019.

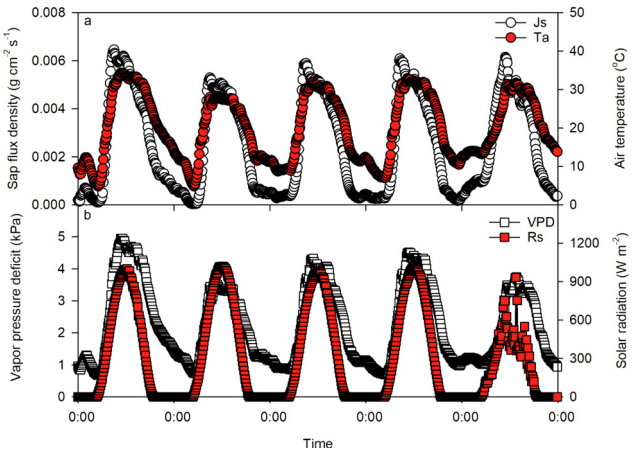

Fig. 4. Diurnal course of sap flux densities (J_s) during five consecutive days (from May 6 to May 10 in 2018) and the corresponding air temperature, vapor pressure deficit, and solar radiation for the sampled trees.

June, July and September of 2019, but this trend was reversed in the other months, irrespective of canopy interception and understory transpiration (Table 2).

3.3. Relationships between environmental variables and canopy transpiration

The daily E_c exhibited an exponentially saturating response to VPD and tended to level off at higher values of VPD, e.g., > 1.5 kPa during the measurement period (Fig. 6a). In addition, the daily E_c significantly increased with increasing R_s in both years, and R_s explained 53 % and 73 % of the variation in daily E_c in the growing seasons in 2018 and 2019, respectively (Fig. 6b). The daily E_c increased with increasing ET_o in both years, and ET_o explained 50 % and 74 % of the variation in E_c in the growing seasons in 2018 and 2019, respectively (Fig. 6c). However, there were no significant relationships between the daily E_c and θ in either years (Fig. 6d).

3.4. Canopy conductance and its relationship with VPD

Diurnal variations in the hourly canopy conductance (G_c), decoupling coefficient (Ω), corresponding hourly air temperature (T_a), vapor pressure deficit (VPD), and solar radiation (R_s) on typical sunny days are shown in Fig. 7. The diurnal variations in hourly G_c and Ω followed a unimodal pattern (Fig. 7a), which was closely related to the changes in hourly T_a, VPD, and R_s (Fig. 7b, c and d). The G_c and Ω began to rise after sunrise, increased sharply and reached maximum values approximately 8:00 local time as the T_a, R_s and VPD increased, and

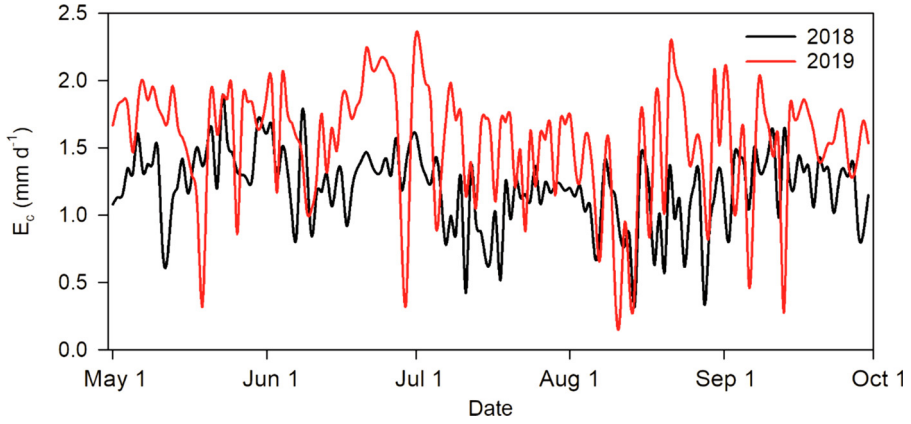

Fig. 5. Dynamics of daily canopy transpiration per unit of ground area (E_c) in poplar plantation during the growing seasons in 2018 and 2019.

Table 2
Water balance component of poplar plantation in 2018 and 2019.

Year	Month	P (mm)	E_c (mm)	E_s (mm)	ΔS (mm)	E_c/P	P-(E_c + ΔS + E_s) (mm)
2018	5	28.4	41.5	32.6	−6.5	1.46	−39.2
	6	79.8	39.4	44.0	0.3	0.49	−3.9
	7	82.0	33.9	57.4	0.9	0.41	−10.2
	8	149.8	31.2	27.8	21.3	0.21	69.5
	9	51.2	38.0	23.0	−9.4	0.74	−0.4
	Total	391.2	184.0	184.8	6.6	0.47	15.8
2019	5	130.5	51.1	34.5	31.7	0.39	13.2
	6	34.9	49.9	49.7	−40.4	1.43	−24.3
	7	106.4	48.2	77.0	21	0.45	−39.8
	8	242.2	41.4	36.0	25.5	0.17	139.3
	9	19.2	45.4	27.0	−36	2.36	−17.2
	Total	533.2	235.9	224.2	−0.6	0.44	73.7

Note: P: Precipitation, E_c: Canopy transpiration, E_s: Soil evaporation, ΔS: change in soil water storage.

subsequently decreased until night, peaking before T_a, VPD and R_s.

The daily G_c averaged 1.4 and 1.9 m s^{-1} during the growing seasons in 2018 and 2019, respectively, ranging from 0.6 to 4.0 m s^{-1} and from 0.8 to 3.9 m s^{-1} (Fig. 8a). In addition, the G_c differed significantly between the two years, with a higher value in 2019 ($t = -7.65$, $P < 0.001$). The Ω value ranged from 0.4 and 0.8 in both growing seasons, with mean values of 0.6 in 2018 and 0.7 in 2019, respectively (Fig. 8b). Additionally, the Ω value was significantly lower in 2018 than in 2019 ($t = -7.46$, $P < 0.001$).

The daily G_c was significantly negatively correlated with VPD in both years, and VPD explained approximately 62 % and 17 % of the variation in G_c in 2018 and 2019, respectively (Fig. 9a). In addition, the slope of the stomatal response to lnVPD (-m) was significantly higher in 2018 than in 2019, but the reference stomatal conductance (G_{cref}) was significantly higher in 2019 than in 2018 (Fig. 9a). Furthermore, the ratio of the stomatal sensitivity to the reference canopy stomatal conductance (-m/G_{cref}) was 0.62 and 0.27 in 2018 and 2019, respectively (Fig. 9a). Moreover, G_c significantly linearly increased with increasing θ in both years, and θ explained approximately 8 % and 13 % of the variation in G_c in 2018 and 2019, respectively (Fig. 9b).

4. Discussion

4.1. Canopy transpiration in the poplar plantation

In the present study, the mean daily E_c for poplar plantations was 1.37 mm d^{-1} during the measurement period, ranging from 0.21 to 2.35 mm d^{-1}, which was within the range reported for other *Populus* spp. plantations (~ 6.7 mm d^{-1}) in other regions (Chang et al., 2006; Petzold et al., 2011; Shen et al., 2015; Bloemen et al., 2017). However, the mean daily E_c of this study was high compared to the values reported for a *Pinus sylvestris* var. *mongolica* plantation at the study site (DBH of 17.1 cm with a density of 404 tree ha^{-1}, 0.75 mm d^{-1}) (Han et al., 2015). In fact, the water availability in the *Pinus sylvestris* var. *mongolica* plantation was higher than that in poplar plantation in this study, e.g., the 8 % mean θ at the 0−100 cm soil depth and 5.0 m groundwater level for the *Pinus sylvestris* var. *mongolica* plantation. Therefore, the higher mean daily canopy transpiration in the present study relative to that in the *Pinus sylvestris* var. *mongolica* plantation was likely due to the higher average sap flux density and sapwood area of poplar (Figs. 1 and 4).

In addition, the total E_c during the growing season was higher in 2019 than in 2018 (Fig. 5), indicating that poplar plantations could significantly increase their E_c in response to increasing precipitation. This finding was consistent with those of other studies showing that increases in canopy transpiration in plants were associated with increasing precipitation in semiarid and arid regions, and vice versa (Chen et al., 2011; Brito et al., 2015; Fang et al., 2019). However, we observed that there was a 28.1 % increase in the total E_c (51.8 mm) in response to a 36 % increase in precipitation (142 mm) in the present study (Table 2). In contrast to our findings, Zheng and Wang (2014) observed only a 13 % increase in E_c in a *Haloxylon ammodendron* plantation in response to a nearly 85 % increase in precipitation during the growing season at the southern edge of the Gurbantünggüt Desert, China. Song et al. (2018) reported that a 61 % precipitation increase brought only a 10 % increase in the E_c of *Pinus sylvestris* var. *mongolica* in a sparse wood grassland in the southern Keerqin Sandy Land. The high magnitude of the increase in E_c in response to an increase in precipitation in this study may indicate a variable water use strategy in poplar trees, that is possibly related to stomatal regulation (Gu et al., 2017). This was supported by the response of canopy conductance to environmental variables at the hourly scale (Fig.7). The stoma opened gradually after sunrise, and canopy transpiration increased rapidly because of the decreasing stomatal control on transpiration (i.e., increasing Ω) (Fig.7). After the peak in G_c, the VPD increased continuously up to a certain value, and the stomatal conductance and transpiration decreased as stomatal control gradually increased, i.e., decreasing Ω (Fig.7). This physiological process imposed a hydraulic limitation on the sap flow path in poplar trees and prevented excessive water losses under high evaporative demands (Chen et al., 2011; Fu et al., 2020).

Irrespective of canopy interception and understory transpiration, water output exceeded water input in most months during the measurement period (Table 2), indicating that trees took up water from the deep soil layer (> 1 m) and/or groundwater. Our results were consistent with the findings of other studies, which reported that trees have the ability to tap water from deeper soil layers and/or groundwater to maintain their transpiration when the topsoil moisture is exhausted

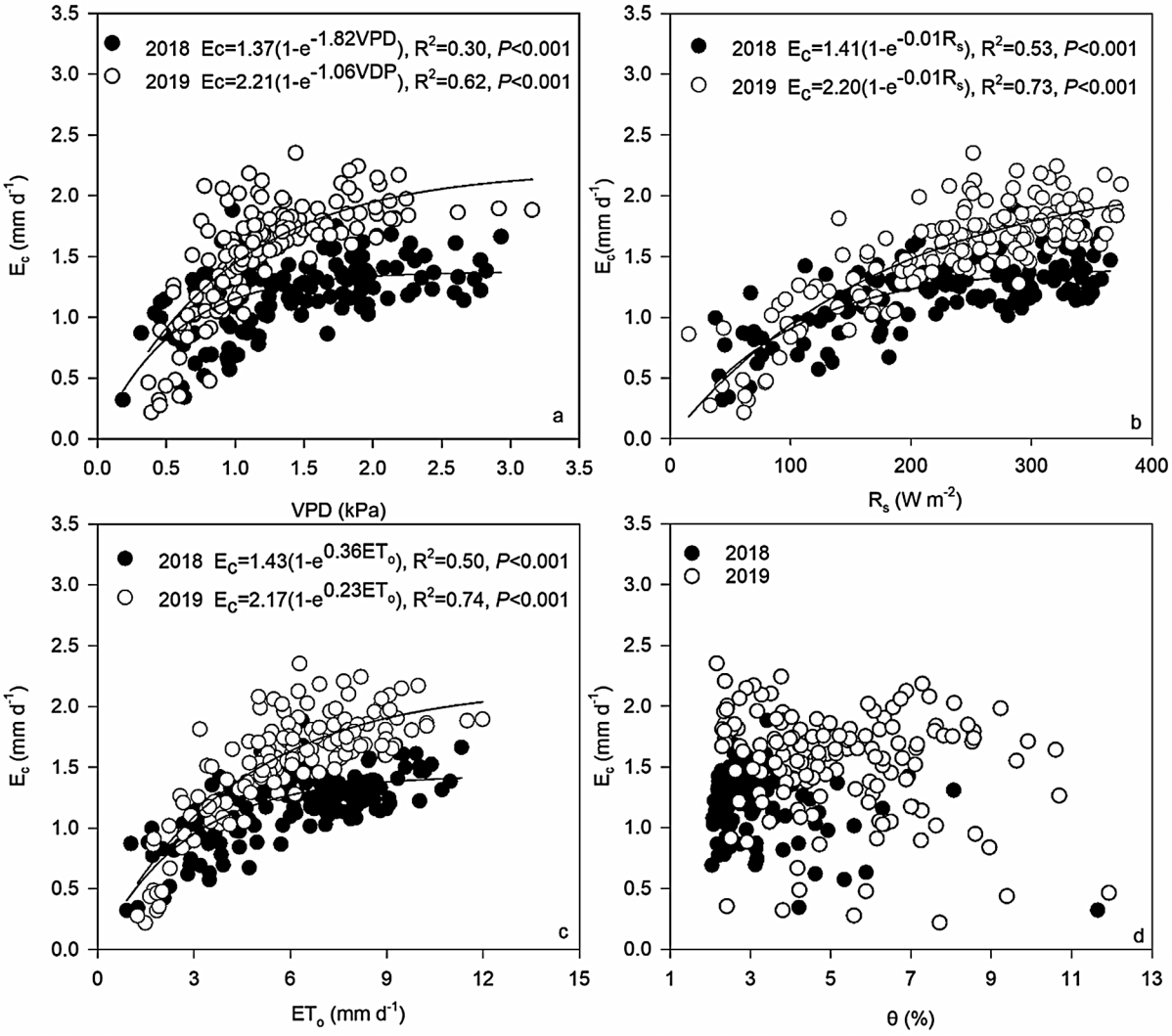

Fig. 6. Relationships between the canopy transpiration (E_c) and daily environmental factors in poplar plantation: vapor pressure deficit (VPD, a), solar radiation (R_s, b), reference evapotranspiration (ET_o, c) and volumetric soil water content (θ, d).

(Brito et al., 2015; Fang et al., 2019). Most of the roots of poplar trees in the Keerqin Sandy Land are distributed within a soil depth range of 100 cm, but the maximum depth of the taproot can reach the groundwater level (Song et al., 2020a). Therefore, poplar trees can take up water from the deep soil layer and/or groundwater when the upper soil water becomes insufficient in the study region. In the same study site, an isotope (deuterium and oxygen) analysis in xylem, soil, precipitation, and groundwater also indicated that the poplar trees used deep soil water (> 1 m) and groundwater in addition to shallow soil water, and the contribution of groundwater to transpiration reached 37.4 % in normal years (Song et al., 2020a). Therefore, poplar trees take up water from the capillary fringe or directly from groundwater, which is an important strategy for coping with soil drought in semiarid sandy environments (Zhang et al., 1999; Fang et al., 2019).

4.2. Environmental control of canopy transpiration in the poplar plantation

In the present study, the daily canopy transpiration increased sharply with increasing vapor pressure deficit and solar radiation, and tended to level off at high levels of vapor pressure deficit in both years (Fig. 6a and b). These findings were consistent with those reported for *Populus* spp. trees and other tree species in other regions (Zhang et al., 1999; Chang et al., 2006; Wieser et al., 2014; Shen et al., 2015; Tie et al., 2017). The saturation of canopy transpiration at high vapor pressure deficit levels is an important adaptive strategy evolved by poplar trees in semiarid sandy environments (Wieser et al., 2014; Brito et al., 2015; Liu et al., 2015; Song et al., 2020b). In addition, more of the variability in the daily canopy transpiration was explained by solar radiation than by the vapor pressure deficit, indicating that canopy transpiration was more controlled by solar radiation than by the vapor pressure deficit on a daily scale. A similar phenomenon was reported by Shen et al. (2015) for *Populus gansuensis* plantations in an arid inland river basin of Northwest China and by Zhang et al. (2013) for *Populus alba* L. × *P. talassica* plantation in the arid desert area. This may be because the canopy was partly decoupled from the atmosphere, and as a result, canopy transpiration became increasingly dependent on solar radiation and less dependent on atmospheric vapor pressure deficit (Wullschleger et al., 1998). This was demonstrated by the Ω values in both years (Fig. 8b, 0.6 and 0.7 in 2018 and 2019, respectively), which approached one (Xu et al., 2018). The extent of the E_c variation explained by ET_o was no higher than that explained by R_s (Fig. 6), which further verified that solar radiation is the main driver of canopy transpiration for poplar. Furthermore, clear relationships between the daily canopy transpiration and soil moisture were not found in either year (Fig. 6d); that is consistent with other studies in which there was no significant relationship between canopy transpiration in plantations and soil moisture on a daily scale (Jiao et al., 2016; Wang et al., 2017; Zhang et al., 2018a). The lack of a significant relationship between soil

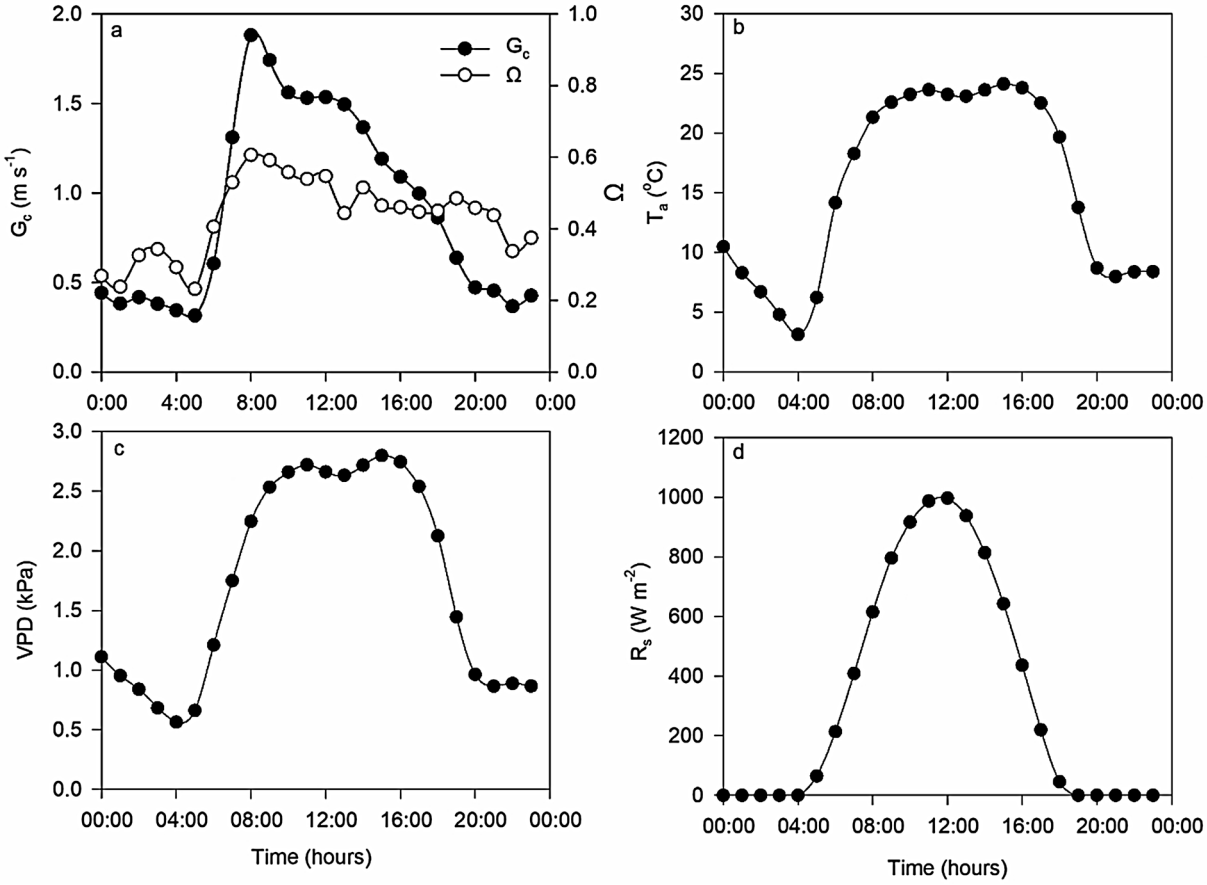

Fig. 7. Diurnal variations in hourly canopy conductance (G_c, a), decoupling coefficient (Ω, a) and the corresponding hourly air temperature (T_a, b), vapor pressure deficit (VPD, c), and solar radiation (R_s, d) in typical sunny days.

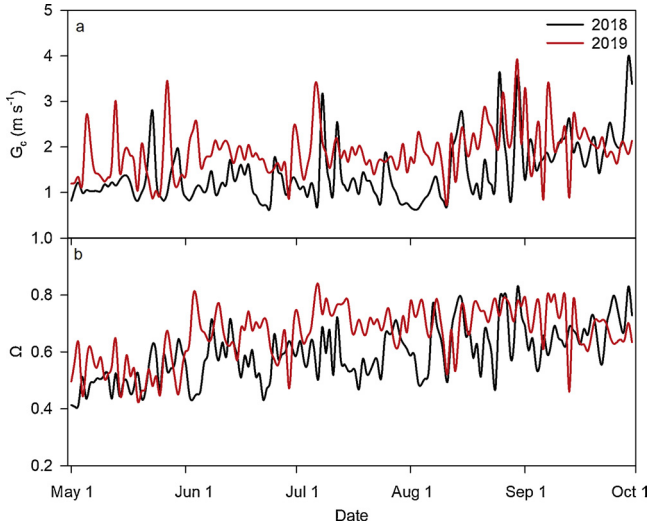

Fig. 8. Dynamics of daily canopy conductance (G_c) and decoupling coefficient (Ω) in the poplar plantation during the growing seasons in 2018 and 2019.

moisture and canopy transpiration on a daily scale might be because seasonal variation weakened the effect of soil moisture on stomatal conductance during the growing seasons (Liu et al., 2017b; Song et al., 2020b). In addition, the utilization of deep soil water (> 1.0 m) and/or groundwater by poplar trees also contributes to weakening this effect (Brito et al., 2015; Song et al., 2020b).

Tree transpiration was regulated by stomatal conductance. The lower G_c in 2018 than in 2019 (Fig. 8a) indicated that trees reduced G_c in response to a decrease in precipitation and soil moisture. This was because the hydraulic resistance between soil and root systems increased as soil water availability decreased, which prevented water movement from the soil to the plant leaves and subsequently resulted in stomatal closure (Tognetti et al., 2009; Li et al., 2016). This was also supported by the positive relationships between G_c and θ in both years (Fig. 9b). In addition, we found that the ratio of stomatal sensitivity to reference canopy stomatal conductance (-m/G_{cref}) for the poplar trees decreased from 0.62 in 2018 to 0.27 in 2019. Generally, the ratio of stomatal sensitivity to reference canopy stomatal conductance (-m/G_{cref}) is approximately 0.6 across a large range of species and environmental conditions, indicating the stomatal regulation of water potential to prevent xylem cavitation (isohydric strategy). Nevertheless, the ratio is lower than 0.6 as a result of trees that exhibit less strict water potential regulation (Oren et al., 1999; Ewers et al., 2005; Naithani et al., 2012). Therefore, our results indicate that the poplar trees showed relatively strict stomatal regulation in 2018 (Igarashi et al., 2015), whereas they showed relatively less strict stomatal regulation of water loss (more anisohydric) in 2019 (Oren et al., 1999; Ogle and Reynolds, 2002). The shift from relatively more to less strict stomatal regulation from normal to wet years in poplar trees in the present study may indicate that the trees showed flexible stomatal regulation of transpiration (Domec and Johnson, 2012). This was also demonstrated by Ω values, which changed from 0.6 in 2018 to 0.7 in 2019 (Fig. 8b).

4.3. Implications for forest and water management

In the present study, precipitation could not satisfy the high transpiration demand of the poplar plantation; therefore, trees took up

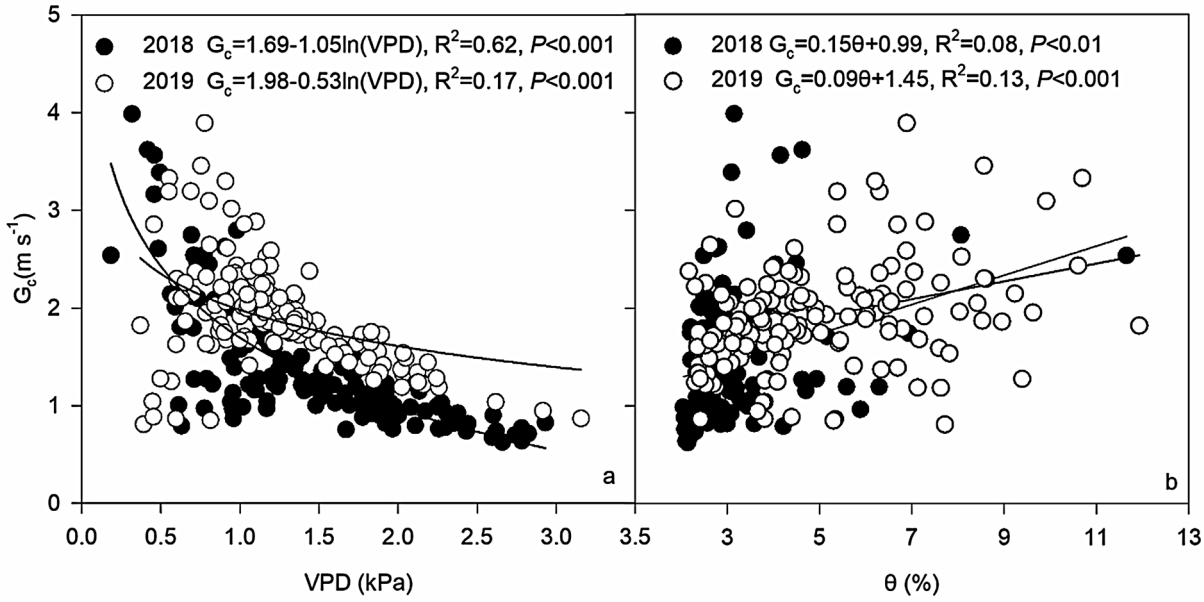

Fig. 9. Canopy conductance (G_c) relationships with vapor pressure deficit (VPD) and volumetric soil water content (θ) in the poplar plantation during the growing seasons in 2018 and 2019.

water from the deep soil layer (> 1.0 m) and from groundwater. However, in the study region, precipitation exhibits strong interannual variations, and extremely low precipitation (approximately half of the long-term mean value) occurrs at an interval of 15 years. In addition, the groundwater level has gradually declined since the 1950s, with a rate of decrease of 0.7 m every 10 years; in a drought year, the decline in the groundwater level can be especially precipitous (Song et al., 2020a), e.g., it decreased from 6.5 m to 8.3 m during the growing season in 2018 at the study site (data not shown). Most studies have shown that severe and abrupt groundwater level declines may lead to severe water stress for trees, casuing crown dieback or even tree death (David et al., 2013). Therefore, poplar plantations are vulnerable to dieback during extreme drought years with a sharp decline in the groundwater level.

Our findings have important implications for afforestation, forest and water management in this semiarid sandy region. Reforestation with poplar is undoubtedly the most practical means of immobilizing shifting sand dunes due to the fast growth of poplar (Zheng et al., 2012; Song et al., 2020a). However, the poplar trees should be planted where the groundwater level is shallow, so that the groundwater or capillary water will be directly utilized by the trees and thus contribute to maintaining higher transpiration. To maintain the stability of poplar plantations, the tree density should be reduced to lower canopy transpiration and interception and to increase the soil water availability for the remaining trees and thus reduce their dependence on groundwater (Giuggiola et al., 2013; Song et al., 2016). Furthermore, Zheng et al. (2012) reported that the decline in groundwater level in the study region was mainly due to the increase in water use for the expansion of agricultural land and broadleaved forests. Therefore, to maintain the local water balance and the stability of poplar plantations, the area covered by agricultural land and poplar plantations should be reduced or transformed into coniferous forests, shrublands, and grasslands with low water consumption (Zheng et al., 2012; Song et al., 2016).

5. Conclusions

Daily canopy transpiration averaged 1.2 mm d^{-1} and 1.5 mm d^{-1} during the growing seasons in 2018 and 2019. Daily canopy transpiration was more controlled by solar radiation than by the vapor pressure deficit. The trees used deep soil water (> 1.0 m) and groundwater to maintain higher canopy transpiration in most months during the measurement period. Canopy conductance decreased significantly with increasing VPD in both years; however, the sensitivity of canopy conductance to VPD decreased from 0.62 in 2018 to 0.27 in 2019, indicating a shift from more to less strict stomatal regulation. Therefore, poplar plantations are vulnerable to dieback during extreme drought years with the decline in the groundwater level becasue the trees utilized groundwater to maintain higher canopy transpiration rates. To maintain the stability of poplar plantations in this semiarid sandy region, suitable afforestation site selection, thinning and land-use type transformation practices should be adopted.

Declaration of Competing Interest

The authors declare that they have no known competing financial interests or personal relationships that could have appeared to influence the work reported in this paper.

Acknowledgements

This research was supported by grants from the Key Research Program of Frontier Sciences, Chinese Academy of Sciences, China (QYZDJ-SSW-DQC027), the National Nature Science Foundation of China (31770757) and Youth Innovation Promotion Association, Chinese Academy of Sciences, China (2018228). We thank Dr. Lizhong Yu, Dr. Qiaoling Yan, Dr. Kai Yang, Dr. Xiao Zheng, Dr. Tian Gao, Dr. Yirong Sun and Ms. Jinxin Zhang in Division of Ecology and Management for Secondary Forest of Institute of Applied Ecology, Chinese Academy of Sciences, China for their helpful discussion on this manuscript.

References

Allen, R.G., Pereira, L.S., Raes, D., Smith, M., 1998. Crop Evapotranspiration. Guidelines for Computing Crop Water Requirements. FAO, Rome, pp. 56 Irrigation and drainage paper.

Anderegg, W.R.L., Anderegg, L.D.L., Kerr, K.L., Trugman, A.T., 2019. Widespread drought-induced tree mortality at dry range edges indicates that climate stress exceeds species' compensating mechanisms. Glob. Change Biol. 25, 3793–3802.

Ayyoub, A., Er-Raki, S., Khabba, S., Merlin, O., Ezzahar, J., Rodrigueze, J.C., Bahlaoui, A., Chehbouni, A., 2017. A simple and alternative approach based on reference evapotranspiration and leaf area index for estimating tree transpiration in semi-arid

regions. Agric. Water Manage. 188, 61–68.
Bloemen, J., Fichot, R., Horemans, J.A., Broeckx, L.S., Verlinden, M.S., Zenone, T., Ceulemans, R., 2017. Water use of a multigenotype poplar short-rotation coppice from tree to stand scale. Bioenergy 9, 370–384.
Bosch, D.D., Marshall, L.K., Teskey, R., 2014. Forest transpiration from sap flux density measurements in a Southeastern Coastal Plain riparian buffer system. Agric. For. Meteorol. 187, 72–82.
Brito, P., Lorenzo, J.R., Águeda, M., González-Rodríguez, Morales, D., Wieser, G., Jiménez, M.S., 2015. Canopy transpiration of a semiarid *Pinus canariensis* forest at a treeline ecotone in two hydrologically contrasting years. Agric. For. Meteorol. 201, 120–127.
Campbell, G.S., Norman, J.M., 1998. An Introduction to Environmental Biophysics. Springer, New York, New York, NY.
Chang, X.X., Zhao, W.Z., Zhang, Z.H., Su, Y.Z., 2006. Sap flow and tree conductance of shelter-belt in arid region of China. Agric. For. Meteorol. 138, 132–141.
Chang, X.X., Zhao, W.Z., Liu, H., Wei, X., Liu, B., He, Z.B., 2014. Qinghai spruce (*Picea crassifolia*) forest transpiration and canopy conductance in the upper Heihe River Basin of arid northwestern China. Agric. For. Meteorol. 198–199, 209–220.
Chen, L.X., Zhang, Z.Q., Li, Z.D., Tang, J.W., Caldwell, P., Zhang, W.J., 2011. Biophysical control of whole tree transpiration under an urban environment in Northern China. J. Hydrol. 402, 388–400.
David, T.S., Pinto, C.A., Nadezhdina, N., Kurz-Besson, C., Henriques, M.O., Quilhó, T., Cermak, J., Chaves, M.M., Pereira, J.S., David, J.S., 2013. Root functioning, tree water use and hydraulic redistribution in *Quercus suber* trees: a modeling approach based on root sap flow. For. Ecol. Manag. 307, 136–146.
Di, N., Xi, B.Y., Clothier, B., Wang, Y., Li, G.D., Ji, L.M., 2019. Diurnal and nocturnal transpiration behaviors and their responses to groundwater-table fluctuations and meteorological factors of *Populus tomentosa* in the North China Plain. For. Ecol. Manage. 448, 445–456.
Domec, J.C., Johnson, D.M., 2012. Does homeostasis or disturbance of homeostasis in minimum leaf water potential explain the isohydric versus anisohydric behavior of *Vitis vinifera* L. cultivars? Tree Physiol. 32, 245–248.
Ewers, B.E., Oren, R., Phillips, N., Strömgren, M., Linder, U., 2001. Mean canopy stomatal conductance responses to water and nutrient availabilities in *Picea abies* and *Pinus taeda*. Tree Physiol. 21, 841–850.
Ewers, B.E., Gower, S.T., Bond-Lamberty, B., Wang, C.K., 2005. Effects of stand age and tree species on canopy transpiration and average stomatal conductance of boreal forests. Plant Cell Environ. 28, 660–678.
Fang, W.W., Lu, N., Liu, J.B., Jiao, L., Zhang, Y., Wang, M.Y., Fu, B.J., 2019. Canopy transpiration and stand water balance between two contrasting hydrological years in three typical shrub communities on the semiarid Loess Plateau of China. Ecohydrology 12, e2064.
Flake, S.W., Weisberg, P.J., 2019. Fine-scale stand structure mediates drought-induced tree mortality in pinyon-juniper woodlands. Ecol. Appl. 29, e01831.
Fu, S., Xiao, Y., Luo, Y., Sun, L., Wu, D.S., 2020. Effect of stomatal control on *Populus simonii* Carr stand transpiration in farmland shelterbelt, China's semi-arid region. Agrof. Syst. 94, 719–731.
Gao, X.C., Zhu, Q., Yang, Z.Y., Liu, J.H., Wang, H., Shao, W.W., Huang, G.R., 2018. Temperature dependence of hourly, daily, and event-based precipitation extremes over China. Sci. Rep. 8, 17564.
Ghimire, C.P., Bruijnzeel, L.A., Lubczynski, M.W., Zwartendijk, B.W., Odongo, V.O., Ravelona, M., van Meerveld, H.J.I., 2018. Transpiration and stomatal conductance in a young secondary tropical montane forest: contrasts between native trees and invasive understorey shrubs. Tree Physiol. 38, 1053–1070.
Giuggiola, A., Bugmann, H., Zingg, A., Dobberti, M., Rigling, A., 2013. Reduction of stand density increases drought resistance in xeric Scots pine forests. For. Ecol. Manag. 310, 827–835.
Granier, A., 1987. Evaluation of transpiration in a Douglas-fir stand by means of sap flow measurements. Tree Physiol. 3, 309–320.
Gu, D.X., Wang, Q., Otieno, D., 2017. Canopy transpiration and stomatal responses to prolonged drought by a dominant desert species in Central Asia. Water 9, 404.
Han, H., Zhang, X.L., Dang, H.Z., Xu, G.J., Zhang, B.X., You, G.C., 2015. Study on proper stand density of *Pinus sylvestris* var. *mongolica* plantation in sandy land based on stem sap flow velocity. For. Res. 28, 797–803 (in Chinese with English abstract).
Hoelscher, M., Kern, M.A., Wessolek, G., Nehls, T., 2018. A new consistent sap flow baseline-correction approach for the stem heat balance method using nocturnal water vapour pressure deficits and its application in the measurements of urban climbing plant transpiration. Agric. For. Meteorol. 248, 169–176.
Igarashi, Y., Kumagai, T., Yoshifuji, N., Sato, T., Tanaka, N., Tanaka, K., Suzuki, M., Tantasirin, C., 2015. Environmental control of canopy stomatal conductance in a tropical deciduous forest in northern Thailand. Agric. For. Meteorol. 202, 1–10.
Jarvis, P.G., McNaughton, K.G., 1986. Stomatal control of transpiration: scaling up from leaf to region. Adv. Ecol. Res. 15, 1–49.
Ji, Y.H., Zhou, G.S., Li, Z.S., Wang, S.D., Zhou, H.L., Song, X.Y., 2020. Triggers of widespread dieback and mortality of poplar (*Populus* spp.) plantations across northern China. J. Arid Environ. 174, 104076.
Jiao, L., Lu, N., Sun, G., Ward, E.J., Fu, B.J., 2016. Biophysical controls on canopy transpiration in a black locust (*Robinia pseudoacacia*) plantation on the semi-arid Loess Plateau, China. Ecohydrology 9, 1068–1081.
Kumagai, T., Saitoh, T.M., Sato, Y., Morooka, T., Manfroi, O.J., Kuraji, K., Suzuki, M., 2004. Transpiration, canopy conductance and the decoupling coefficient of a lowland mixed dipterocarp forest in Sarawak, Borneo: dry spell effects. J. Hydrol. 287, 237–251.
Leo, M., Oberhuber, W., Schuster, R., Grams, T.E.E., Matyssek, R., Wieser, G., 2013. Evaluating the effect of plant water availability on inner alpine coniferous trees based on sap flow measurements. Eur. J. For. Res. 133, 691–698.
Li, W., Si, J.H., Yu, T.F., Li, X.Y., 2016. Response of *Populus euphratica* Oliv. sap flow to environmental variables for a desert riparian forest in the Heihe River Basin, Northwest China. J. Arid Land 8, 591–603.
Li, M.Y., Fang, L.D., Duan, C.Y., Cao, Y., Yin, H., Ning, Q.R., Hao, G.Y., 2020. Greater risk of hydraulic failure due to increased drought threatens pine plantations in Horqin Sandy Land of northern China. For. Ecol. Manag. 461, 117980.
Liu, H.J., Cohen, S., Lemcoff, J.H., Israeli, Y., Tanny, J., 2015. Sap flow, canopy conductance and microclimate in a banana screenhouse. Agric. For. Meteorol. 201, 165–175.
Liu, W.F., Wu, J.P., Fan, H., Duan, H.B., Li, Q., Yuan, Y.H., Zhang, H., 2017a. Estimations of evapotranspiration in an age sequence of Eucalyptus plantations in subtropical China. PLoS One 12, e0174208.
Liu, X., Zhang, B., Zhuang, J.Y., Han, C., Zhai, L., Zhao, W.R., Zhang, J.C., 2017b. The relationship between sap flow density and environmental factors in the Yangtze River Delta region of China. Forests 8, 74.
Lu, P., Urban, L., Zhao, P., 2004. Granier's thermal dissipation probe (TDP) method for measuring sap flow in trees: theory and practice. Acta Bot. Sin. 46, 631–646.
Manzoni, S., Katul, G., Porporato, A., 2014. A dynamical system perspective on plant hydraulic failure. Water Resour. Res. 50, 5170–5183.
Matusick, G., Ruthrof, K.X., Kala, J., Brouwers, N.C., Breshears, D.D., Hardy, G.E.S.J., 2018. Chronic historical drought legacy exacerbates tree mortality and crown dieback during acute heatwave-compounded drought. Environ. Res. Lett. 13, 095002.
McDowell, N.G., White, S., Pockman, W.T., 2008. Transpiration and stomatal conductance across a steep climate gradient in the southern Rocky Mountains. Ecohydroloy 1, 193–204.
Monteith, J.L., Unsworth, M.H., 2013. Mass transfer: (ii) Particles—principles of environmental physics (fourth edition)—chapter 12. Princ. Environ. Phys. 199–216.
Muñoz-Villers, L.E., Holwerda, F., Alvarado-Barrientos, M.S., Geissert, D.R., Dawson, T.E., 2018. Reduced dry season transpiration is coupled with shallow soil water use in tropical montane forest trees. Oecologia 188, 303–317.
Naithani, K.J., Ewers, B.E., Pendall, E., 2012. Sap flux-scaled transpiration and stomatal conductance response to soil and atmospheric drought in a semi-arid sagebrush ecosystem. J. Hydrol. 464–465, 176–185.
Ogle, K., Reynolds, J.F., 2002. Desert dogma revisited: coupling of stomatal conductance and photosynthesis in the desert shrub Larrea tridentata. Plant Cell Environ. 25, 909–921.
Oren, R., Sperry, J.S., Katul, G.G., Pataki, D.E., Ewers, B.E., Phillips, N., Schäfer, K.V.R., 1999. Survey and synthesis of intra- and interspecific variation in stomatal sensitivity to vapour pressure deficit. Plant Cell Environ. 22, 1515–1526.
Otieno, D., Li, Y.L., Ou, Y.X., Cheng, J., Liu, S.Z., Tang, X.L., Zhang, Q.M., Jung, E.Y., Zhang, D.Q., Tenhunen, J., 2014. Stand characteristics and water use at two elevations in a sub-tropical evergreen forest in southern China. Agric. For. Meteorol. 194, 155–166.
Pasqualotto, G., Carraro, V., Menardi, R., Anfodillo, T., 2019. Calibration of Granier-Type (TDP) sap flow probes by a high precision electronic potometer. Sensors 19, 2419.
Petzold, R., Schwärzel, K., Feger, K.H., 2011. Transpiration of a hybrid poplar plantation in Saxony (Germany) in response to climate and soil conditions. Eur. J. For. Res. 130, 695–702.
Rana, G., Lorenzi, F.D., Mazza, G., Martinelli, N., Muschitiello, C., Ferrara, R.M., 2020. Tree transpiration in a multi-species Mediterranean garden. Agric. For. Meteorol. 280, 107767.
Sánchez-Costa, E., Poyatos, R., Sabaté, S., 2015. Contrasting growth and water use strategies in four co-occurring Mediterranean tree species revealed by concurrent measurements of sap flow and stem diameter variations. Agric. For. Meteorol. 207, 24–37.
Shen, Q., Gao, G.Y., Fu, B.J., Lu, Y.H., 2015. Sap flow and water use sources of shelter-belt trees in an arid inland river basin of Northwest China. Ecohydrology 8, 1446–1458.
Sommer, R., de Abreu Sá, T.D., Vielhauer, K., de Araújo, A.C., Fölster, H., Vlek, P.L.G., 2002. Transpiration and canopy conductance of secondary vegetation in the eastern Amazon. Agri. For. Meteorol. 112, 103–121.
Song, L.N., Zhu, J.J., Li, M.C., Zhang, J.X., 2016. Water use patterns of *Pinus sylvestris* var. *mongolica* trees of different ages in a semiarid sandy lands of Northeast China. Environ. Exp. Bot. 129, 94–107.
Song, L.N., Zhu, J.J., Li, M.C., Zhang, J.X., Wang, K., Lü, L.Y., 2020a. Comparison of water-use patterns for non-native and native woody species in a semiarid sandy region of Northeast China based on stable isotopes. Environ. Exp. Bot. 174, 103923.
Song, L.N., Zhu, J.J., Zheng, X., Wang, K., Lü, L.Y., Zhang, X.L., Hao, G.Y., 2020b. Transpiration and canopy conductance dynamics of *Pinus sylvestris* var. *mongolica* in its natural range and in an introduced region in the sandy plains of Northern China. Agric. For. Meteorol. 218, 107830.
Song, L.N., Zhu, J.J., Li, M.C., Zhang, J.X., Zheng, X., Wang, K., 2018. Canopy transpiration of *Pinus sylvestris*var. *mongolica* in a sparse wood grassland in the semiarid sandy region of Northeast China. Agric. For. Meteorol. 250–251, 192–201.
Su, F.L., Zhao, H.K., Guo, C.J., Jia, Y.H., 2010. Characters of sap flow of *Populus* × *xiaozhuanica* and its relations with environment factors. Acta Agric. Boreali-occidentalis Sin. 19, 164–173 (in Chinese with English abstract).
Tie, Q., Hu, H.C., Tian, F.Q., Guan, H.D., Lin, H., 2017. Environmental and physiological controls on sap flow in a subhumid mountainous catchment in North China. Agric. For. Meteorol. 240–241, 46–57.
Tognetti, R., Giovannelli, A., Lavini, A., Morelli, G., Fragnito, F., d'Andria, R., 2009. Assessing environmental controls over conductance through the soil-plant-atmosphere continuum in an experimental olive tree plantation of southern Italy. Agric. For. Meteorol. 149, 1229–1243.
Tsuruta, K., Komatsu, H., Kume, T., Otsuki, K., Kosugi, Y., Kosugi, K., 2019. Relationship between stem diameter and transpiration for Japanese cypress trees: implications for estimating canopy transpiration. Ecohydrology 12, e2097.

Tu, J., Wei, X.H., Huang, B.B., Fan, H.B., Jian, M.F., Li, W., 2019. Improvement of sap flow estimation by including phenological index and time-lag effect in back-propagation neural network models. Agric. For. Meteorol. 276–277, 107608.
Ungar, E.D., Rotenberg, E., Raz-Yaseef, N., Cohen, S., Yakir, D., Schiller, G., 2013. Transpiration and annual water balance of Aleppo pine in a semiarid region: implications for forest management. For. Ecol. Manage. 298, 39–51.
Urban, J., Ingwers, M.W., McGuire, M.A., Teskey, R.O., 2017. Increase in leaf temperature opens stomata and decouples net photosynthesis from stomatal conductance in *Pinus taeda* and *Populus deltoides*×*Nigra*. J. Exp. Bot. 68, 1757–1767.
Wang, H.L., Tetzlaff, D., Dick, J.J., Soulsby, C., 2017. Assessing the environmental controls on Scots pine transpiration and the implications for water partitioning in a boreal headwater catchment. Agric. For. Meteorol. 240–241, 58–66.
Wang, S., Fan, J., Ge, J.M., Wang, Q.M., Fu, W., 2019. Discrepancy in tree transpiration of *Salix matsudana*, *Populus simonii* under distinct soil, topography conditions in an ecological rehabilitation area on the Northern Loess Plateau. For. Ecol. Manag. 432, 675–685.
Wieser, G., Leo, M., Oberhuber, W., 2014. Transpiration and canopy conductance in an inner alpine Scots pine (*Pinus sylvestris*) forest. Flora 209, 491–498.
Wullschleger, S.D., Meinzer, F.C., Vertessy, R.A., 1998. A review of whole-plant water use studies in trees. Tree Physiol. 18, 499–512.
Xu, S.Q., Yu, Z.B., Zhang, K., Ji, X.B., Yang, C.G., Sudicky, E.A., 2018. Simulating canopy conductance of the *Haloxylon ammodendron* shrubland in an arid inland river basin of northwest China. Agric. For. Meteorol. 249, 22–34.
Zeppel, M.J.B., Macinnis-Ng, C.M.O., Yunusa, I.A.M., Whitley, R.J., Eamus, D., 2008. Long term trends of stand transpiration in a remnant forest during wet and dry years. J. Hydrol. 349, 200–213.
Zhang, H.P., Morison, J.I.L., Simmonds, L.P., 1999. Transpiration and water relations of poplar trees growing close to the water table. Tree Physiol. 19, 563–573.
Zhang, Q.Y., Jia, X.X., Shao, M.G., Zhang, C.C., Li, X.D., Ma, C.K., 2018a. Sap flow of black locust in response to short-term drought in southern Loess Plateau of China. Sci. Rep. 8, 6222.
Zhang, Z.Z., Zhao, P., Zhao, X.H., Zhou, J., Zhao, P.Q., Zeng, X.M., Hu, Y.T., Ouyang, L., 2018b. The tree height-related spatial variances of tree sap flux density and its scale-up to stand transpiration in a subtropical evergreen broadleaf forest. Ecohydrology 11, e1979.
Zhang, J., Li, X.F., Li, J.G., Wang, H., Huang, C.T., Min, S.J., Li, G., Zhang, F.H., Tian, X., Kong, J., 2013. Sap flow dynamics of *Populus albaL.*×*P. Talassica* plantation in arid desert area. Acta Ecol. Sin. 33, 5655–5660 (in Chinese with English abstract).
Zhang, Z.Z., Zhao, P., McCarthy, H.R., Zhao, X.H., Niu, J.F., Zhu, L.W., Ni, G.Y., Ouyang, L., Huang, Y.Q., 2016. Influence of the decoupling degree on the estimation of canopy stomatal conductance for two broadleaf tree species. Agric. For. Meteorol. 221, 230–241.
Zhang, H.D., Wei, W., Chen, L.D., Wang, L.X., 2017. Effects of terracing on soil water and canopy transpiration of *Pinus tabulaeformis* in the Loess Plateau of China. Ecol. Eng. 102, 557–564.
Zheng, C.L., Wang, Q., 2014. Seasonal and annual variation in transpiration of a dominant desert species, *Haloxylon ammodendron*, in Central Asia up-scaled from sap flow measurement. Ecohydrology 8, 948–960.
Zheng, X., Zhu, J.J., Yan, Q.L., Song, L.N., 2012. Effects of land use changes on the groundwater table and the decline of *Pinus sylvestris* var. *mongolica* plantations in southern Horqin Sandy Land, Northeast China. Agric. Water Manage. 109, 94–106.
Zhu, J.J., Fan, Z.P., Zeng, D.H., Jiang, F.Q., Takeshi, M., 2003. Comparison of stand structure and growth between plantation and natural forests of *Pinus sylvestris* var. *mongolica* on sandy land. J. For. Res. 14, 103–111.
Zhu, J.J., Li, F.Q., Xu, M.L., Kang, H.Z., Xu, D.Y., 2008. The role of ectomycorrhizal fungi in alleviating pine decline in semiarid sandy soil of northern China: an experimental approach. Ann. For. Sci. 65, 1–12.